

Article

An Integrated Approach Supporting Remediation of an Aquifer Contaminated with Chlorinated Solvents by a Combination of Adsorption and Biodegradation

Paolo Ciampi ^{1,*} , Carlo Esposito ¹ , Paolo Viotti ² , Jacopo Boaga ³, Giorgio Cassiani ³ and Marco Petrangeli Papini ⁴ 

¹ Department of Earth Science, Sapienza University of Rome, Piazzale Aldo Moro 5, 00185 Rome, Italy; carlo.esposito@uniroma1.it

² Department of Civil, Building and Environmental Engineering, Sapienza University of Rome, Via Eudossiana 18, 00184 Rome, Italy; paolo.viotti@uniroma1.it

³ Department of Geosciences, University of Padua, Via Gradenigo 6, 35131 Padua, Italy; jacopo.boaga@unipd.it (J.B.); giorgio.cassiani@unipd.it (G.C.)

⁴ Department of Chemistry, Sapienza University of Rome, Piazzale Aldo Moro 5, 00185 Rome, Italy; marco.petrangelipapini@uniroma1.it

* Correspondence: paolo.ciampi@uniroma1.it; Tel.: +39-348-9194-607

Received: 30 July 2019; Accepted: 11 October 2019; Published: 14 October 2019



Abstract: Hydrogeological uniqueness and chemical-physical peculiarities guide the contamination dynamics and decontamination mechanisms in the environmental arena. A single composite geodatabase, which integrates geological/hydrological, geophysical, and chemical data, acts as a “cockpit” in the definition of a conceptual model, design of a remediation strategy, implementation, near-real-time monitoring, and validation/revision of a pilot test, and monitoring full-scale interventions. The selected remediation strategy involves the creation of “reactive” zones capable of reducing the concentration of chlorinated solvents in groundwater through the combined action of adsorption on micrometric activated carbon, which is injected into the aquifer, and degradation of organic contaminants, stimulating the dechlorinating biological activity by the addition of an electron donor. The technology is verified through a pilot test, to evaluate the possibility of scaling up the process. The results of post-treatment monitoring reveal abatement of the concentration of chlorinated solvents and intense biological dechlorination activity. Achieving the remediation objectives and project closure is based on the integration of multidisciplinary data using a multiscale approach. This research represents the first completed example in European territory of remediation of an aquifer contaminated with chlorinated solvents by a combination of adsorption and biodegradation.

Keywords: groundwater contamination; remediation; three-dimensional (3D) hydrogeophysical model; geodatabase; pilot test; biodegradation

1. Introduction

Groundwater contamination by dense non-aqueous phase liquids (DNAPLs), such as chlorinated solvents, is increasingly recognized as a serious environmental problem [1]. Chlorinated solvents, including trichloroethylene (TCE) and tetrachloroethylene (PCE), are the most important subclass of DNAPLs [2] due to their widespread use in the electronics, chemical, dry cleaning, and metal fabrication industries [3]. The physical and chemical properties of DNAPLs, aside from their relatively low solubility [4], high specific gravity [5], and tendency to remain adsorbed to organic and fine-grained materials [6], make them difficult to locate and characterize in the subsurface [7], and this can impact the effectiveness of conventional remedial technologies [8].

Over the last decade, in situ application of activated carbon-based amendments has emerged as a promising remedial technology for the cleanup of subsurface organic contaminants such as chlorinated solvents [9,10]. The technology involves a combination of adsorption, which has been extensively characterized and well understood, and degradation [9–11]. The combination of these two processes is proposed to be more effective than conventional in situ remedial technologies that solely rely on degradation [10]. Despite the rapidly increasing number of field-scale applications, unanswered questions remain regarding the effectiveness and persistence of contaminant degradation, especially biodegradation [10]. In the present work, a colloidal activated carbon, PlumeStop™ (Regenesis), was considered as a versatile adsorbent for in situ groundwater remediation [11]. PlumeStop™ combines sorption-based contaminant removal with accelerated biodegradation [10]. The activated carbon-based amendment was co-injected with an electron donor (HRC™, Regenesis) to provide initial biostimulation of the treatment [12]. The selection and deployment of appropriate technologies for the remediation strategy were based on initial characterization activities [13]. In environmental issues, geology-related factors control the migration of contaminant plumes and influence the effectiveness of remediation technologies [14]. The performance of activated carbon-based amendments applied in situ is heavily affected by subsurface heterogeneity and the resulting uncertainty in the delivery and distribution of reagents [10]. The high-resolution characterization of underground geological heterogeneities and the integration of information represent key elements for characterization refinement, remediation design, optimization of intervention, and performance monitoring [15]. The combination of different prospecting techniques provides additional and precious information by capturing the complexity of geological heterogeneity and allowing data spatialization [16]. Conventional site investigation relies on intrusive methods, such as borehole drilling and cone penetration tests [17]. These techniques provide only point information concerning the subsurface, with possible effects of spatial aliasing [18,19]. In addition, drilling can potentially spread contamination by opening DNAPL migration pathways through low-permeability zones [20]. Together with intrusive techniques, geophysical methods are now beginning to be applied to DNAPL contamination problems, both to assist in situ characterization and to monitor remediation processes [21]. Geophysical techniques have the advantage of reducing the need for intrusive investigations [20] and can provide spatially continuous information regarding the subsurface structure [16]. Some geophysical techniques can focus with an adequate resolution (meter) on the first meters to tens of meters of subsoil. In addition, possible links exist between relevant measured physical quantities and hydrological and environmental quantities of interest for contaminated site characterization [19]. The technique considered in this study is electrical resistivity tomography (ERT). According to previous studies, this technique can discriminate geological site structures [22], hydrogeology [23], contaminated materials, and biogeochemical processes [24] based on altered electrical properties. This research emphasizes the importance of integrated use of geological, hydrogeological, chemical, and geophysical data to achieve high-resolution characterization of underground geological heterogeneity, aquifers, and contaminated areas [25].

The proper collection, storage, representation, and integration of geothematic data from different sources are key aspects in defining reliable remediation strategies for contaminated sites [14]. The creation of a "4D" geographical database (which also considers the time factor) enables the integrated management, representation, and analysis of different data (geological, hydrogeological, geophysical, and chemical) [26]. The multitemporal and multidisciplinary geodatabase assumes the role of an effective "near real time" decision support system (DSS) [26–28] able to manage and release data from characterization to implementation of the technique. The 3D georeferenced model extracts useful information for the decision-making process quickly and in a versatile way. The hydrogeological uniqueness and chemical peculiarities orient the selection of a remediation technology and identification of the application points [14]. The selected remediation technology was verified through a pilot test, which was monitored through ERT in near real time, with water and soil sampling, to obtain technical and operational information for optimization of the intervention procedures on a larger scale. Based on the satisfactory results of laboratory investigations (microbiological and microcosm tests) [29–31], a

field test was designed and implemented as the final step of the evaluation process, which led to the selection of an appropriate remediation technology according to the hydrogeochemical peculiarities of the site [15].

The possibility of scaling up the process was evaluated using the pilot test. Full-scale results provide information on the long-term trend of the groundwater treatment onsite. The work illustrates the remediation measures adopted and the results of post-treatment monitoring for a period of two years. The results that led to project closure derive from the integration of multidisciplinary data, using a multiscale approach. This research represents the first completed example in European territory of remediation of an aquifer contaminated with chlorinated solvents by a combination of adsorption and biodegradation.

2. Materials and Methods

At the contaminated site of the new high-speed railway station of Bologna, Italy, a large amount of slightly contaminated soil (~1,000,000 m³) was excavated to create the new underground station. The excavation activities for construction of the structure that houses the station involved the removal of land attributable to shallow and intermediate aquifers. Corresponding to the excavation, a bypass system equipped with activated carbons for the treatment of groundwater was implemented prior to our intervention. The management of a large amount of heterogeneous data supports the entire remediation project, from the characterization phase to the application of interventions [15]. A large amount of multithematic data was stored and centralized in an integrated information management and analysis platform. The integrated geodatabase represents an effective near-real-time decision support system (DSS) able to manage and release data during the different remediation phases, from characterization to technique implementation, in the field test and at full scale [26]. The hydrogeological model analysis and selection of a remediation technology utilized multiscale and multiphase approaches [32]. In the first phase, the main hydrogeological characteristics surrounding the new high-speed railway station at full scale were detected. In the second phase, starting from the hydrogeological conceptual model obtained from the first one, the analysis focused on the pilot test area, increasing the observation scale to analyze in more detail the effects of geological heterogeneity in the first intervention area. The advanced geological modeling at both scales followed the reworking of stratigraphic data and archiving them in the geodatabase. In the study area, 47 stratigraphic logs from boreholes drilled between 2005 and 2014 were available. A further 17 boreholes were drilled during our activity (2016), to refine the geological model and take soil samples for laboratory tests. Geological surveys and laboratory analyses identified the lithotechnical units and evaluated the permeability of the stratigraphic horizons present in the station subsoil [33]. For this work, the stratigraphic data were reinterpreted and homogenized for a hydrogeological perspective, i.e., the various stratigraphic levels were merged or differentiated according to grain size and, hence, permeability [34]. The subsoil geological structure was subdivided in accordance with the groundwater circulation scheme. Permeability was evaluated via small-scale in situ tests (5 Lefranc tests) as a function of particle size, and through permeability tests in triaxial cells. Twenty-one soil samples were collected to perform particle size tests [35], determine Atterberg limits [36], and assess water content [37]. These analyses were performed at the Applied Geology Laboratory of the University of Rome (La Sapienza). The data acquired were organized according to a hydrostratigraphic criterion [34]. The georeferencing of the previous data and the new periodic measurements allowed hydrogeological structure modeling and reconstruction of the groundwater circulation scheme. The evaluation of hydrodynamic parameters enabled us to quantify the velocity of groundwater flow [38]. The hydrogeological setting was assembled based on a piezometric network consisting of 61 measurement points, 29 and 32 piezometers intercepting the shallow and intermediate aquifers, respectively, were considered. To strengthen the geological model, which arose from the interpolation of punctual data, geophysical investigations were conducted by performing three ERT [39] profiles covering the pilot test area. The ERT profile acquisition was aimed at refining the conceptual geological model in the first application area. The site imposed significant logistic limitations. Given

the presence of the nearby railroad in the west and construction works in the east, it was possible to deploy lines having sufficient length only in the north–south direction. Note that the ERT line geometry determines the maximum depth of investigation, which can be estimated to reach one-quarter to one-fifth of the line length [40]. In the case considered here, it was possible to deploy only 72 electrodes with 1 m spacing along 3 parallel lines, and thus we could only reach a depth of about 15 m. This implies that the ERT investigation only covered the shallow aquifer. The electrode configuration employed in electrical prospecting was a dipole–dipole array, and more precisely a skip-4 dipole–dipole, i.e., the dipole size equals 5 times the electrode spacing, or 5 m in total. The acquisition was conducted using a Syscal Pro 72, produced by Iris Instruments. A full direct and reciprocal acquisition scheme was used, for a total of about 5000 measurements along each line, and an acquisition time in the range of 30 minutes. The direct-reciprocal acquisition (i.e., exchange of current and potential dipoles) was necessary to assess the measurement error [41], which in turn was needed in the inversion process. For the data inversion, and consequently the production of imaging results, we used the open software ProfileR, provided by A. Binley [42]. The error threshold for resistance measurements and inversions was consistently fixed at 10%, which is a value compatible with the challenging electrical contact conditions posed by the partially paved soil surface and the need to drill holes for the electrodes through it. The evolution of the groundwater contamination status was reproduced based on a chemical analysis of water sampled in the monitoring network. A total of 180 monitoring campaigns were conducted in the period 2005–2019. Several thematic maps were produced by considering some key contaminants, which were correlated with the previously ascertained state of contamination. The concentration values were compared to the Italian threshold limits (CSC), the limits between each class correspond to multiples of the CSC value for each contaminant. We created thematic maps for the most relevant parameters, TCE and PCE concentration values, to visualize the evolution of groundwater pollution and identify intervention areas. To investigate the contamination dynamics, we grouped the data, taking into account the different phases of construction of the train station. For each parameter and each considered aquifer formation, we produced contour maps for the following phases:

1. Preoperative (October 2004 to May 2006)
2. Preliminary excavation (May 2006 to October 2009)
3. Excavation (October 2009 to August 2011)
4. Post-excavation (August 2011 to January 2013)
5. Postoperative (January 2013 to December 2014)

Following an accurate reconstruction of the qualitative status evolution of the 2 aquifers, the laboratory tests (microbiological and microcosm tests) were aimed at evaluating spontaneous dechlorination activity [29–31]. The purpose of the microbiological and microcosm chemical tests (not shown here) was to verify possible usage of an injectable colloidal activated carbon (PlumeStop®, Regenesis) at the identified contamination spots both for removal by adsorption of contaminants from the dissolved phase and for possible acceleration of biological processes of reductive dechlorination [10,11]. Based on the results obtained from the site characterization and microbiological [31] and microcosm [29,30] studies, a pilot test was designed to optimize the operating conditions at the field scale. The complete multidisciplinary, multiscale, and multitemporal characterization identified the intervention areas and supported the choice of remediation technology to be deployed. The pilot test was intended to ascertain the feasibility of the proposed remediation solution. It was designed in one of the intervention areas to optimize the layout and calibrate the implementation of an optimized full-scale intervention in order to check its efficiency. Time-lapse geophysical surveys and soil and groundwater sampling during pilot testing were intended to prove effective product diffusion in the 2 aquifers. After the PlumeStop™ injection, some surveys were conducted in the pilot test area using direct push (Geoprobe) penetrometers [43]. These investigations were aimed at visually checking the sediment color after injection and collecting soil samples for various analyses and tests. Seven penetrometric surveys were performed to investigate the subsurface to a depth of 10 m.

The sediments subjected to treatment with PlumeStop™ underwent slight color variation, due to the covering of soil particles with activated carbon. During the monitoring activity, a passive groundwater sampling system was installed in some piezometers intercepting the intermediate aquifer. Snap Samplers® (Q.E.D. Environmental Systems, Inc., Dexter, MI, USA) minimize the impact of the sampling process on groundwater chemistry [44]. Groundwater samples were collected using this method after PlumeStop™ injection. Among the monitoring activities, time-lapse geophysical investigations played a specific role. The use of repeated geophysical measurements to highlight changes in the system is state of the art for several hydrological applications but is used relatively scarcely at contaminated sites, particularly during remediation activities [40,45–47]. An ERT profile during pilot testing was acquired to verify the correct product spread in the first application area. The pilot test was conducted in a limited area, with the purpose of optimizing procedures and operational modes of interventions to scale up the process. Analytical monitoring at the sampling points constituting the piezometric network was done to check the effectiveness of the intervention adopted. The results of full-scale intervention provide information on the long-term trend of the groundwater treatment onsite. The multisource and multitemporal data were organized, georeferenced, and stored in a geodatabase, also useful for visualization and data processing. The hydrogeophysical 3D model was reconstructed by means of RockWorks 17 software (RockWare Inc., Golden, CO, USA) [48]. This software enables the acquisition, analysis, visualization, and integration of information from georeferenced data. The data integration and analysis phase involved interpolating and processing the geological, geophysical, and hydrochemical parameters [49,50]. The parameters included the characteristics of stratigraphic horizons, groundwater levels, geophysical information, and the chemical analysis of the sampled water. Data belonging to different scientific spheres were elaborated with the inverse distance weighted geostatistical method [50–52] to obtain an integrated multidisciplinary model. The interpolation of punctual data, performed using the appropriate algorithm, generated 3-dimensional models, which illustrate the spatial distribution of the parameters obtained from all investigations. The combination of these highly complementary data types—geology, hydrogeology, geophysics, geochemistry—enables the production of value-added photorealistic outcrop models, adding new information that can be used to capture the geological uniqueness, contamination dynamics, and performance of the adopted remediation intervention.

3. Results and Discussion

3.1. Geological and Hydrogeological Settings

The outcropping deposits in the Bologna area are characterized by the Quaternary alluvial succession of the Po River Basin, exceeding 300 m in thickness. A subdivision of the Quaternary alluvial succession of the Po River Basin in the Bologna area has been proposed by Lugli et al. [53] and Regione Emilia-Romagna [54]. The Quaternary alluvial sequence shows a periodic alternation of coarse-grained (gravel and sand) and fine-grained (silt and clay) deposits, their repeated alternation represents the main feature of the depositional system [53,54]. In the study area, this arrangement is clearly recognizable: predominantly gravelly-sandy levels (characterized by variable thickness) are separated by silty-clay deposits. Beyond the backfill material, it is possible to distinguish the first level with fine granulometry, consisting of silty clays and clayey silts with thin laminations of very fine sand, followed by a second horizon composed of sands, fine sands with silt, and sandy silts arranged according to a stratigraphic succession. The third level of plastic clays and silty clays underlies the previous ones and covers the fourth stratum of medium sands with heterometric gravels. Below, consistent clays overlap sandy gravels. The lateral and vertical lithological heterogeneity has important implications regarding the variability of subsoil permeability. This alternate structure of high- and low-permeability zones can create preferential pathways for groundwater flow and solute transport [14,32]. For this reason, the geological structure of the subsoil was subdivided based on permeability characteristics, as follows:

1. Backfill (anthropogenic) materials
2. Shallow clays and silts, low-permeability level of separation between backfill materials and shallow aquifer deposits
3. Shallow aquifer
4. Aquiclude 1, a low-permeability level of separation between shallow and intermediate aquifers
5. Intermediate aquifer
6. Aquiclude 2, a low-permeability level of separation between intermediate and deep aquifers
7. Deep aquifer

The subparallel structures that characterize the different horizons are very evident in the three-dimensional lithostratigraphic model (Figure 1), a vertical exaggeration factor was used to mark the lithological steps.

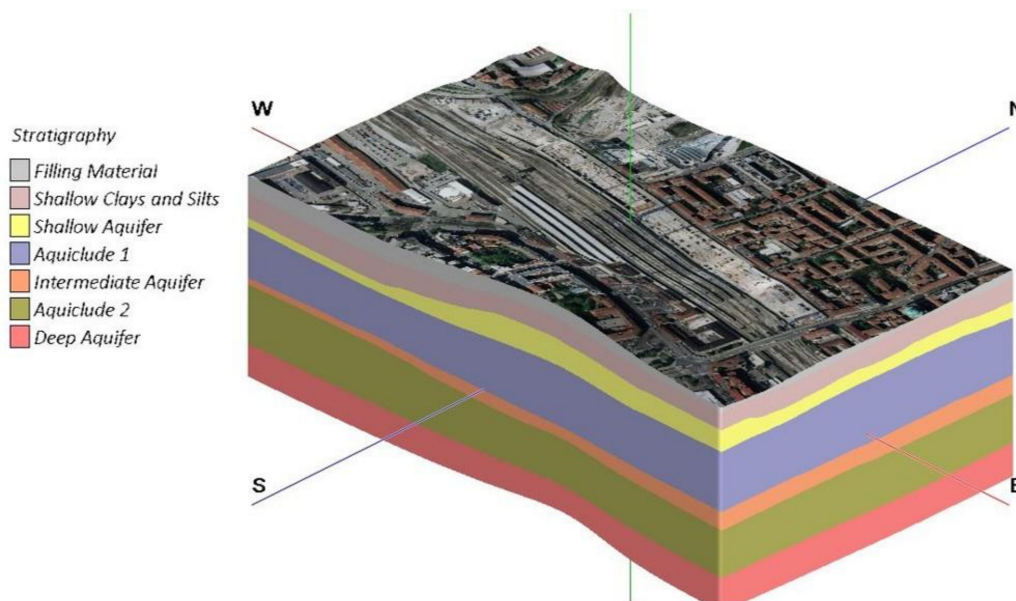


Figure 1. Three-dimensional geological model of the new high-speed railway station of Bologna.

The hydrogeological conceptual model shows the presence of three aquifers separated by low-permeability layers. The shallow and intermediate aquifers are relevant for the contamination issue. The shallow aquifer is composed of deposits with predominantly sandy and sandy-silty grain size. The intermediate aquifer is predominantly composed of gravelly and gravelly-sandy deposits. The shallow aquifer is characterized by variable thickness. The morphology of the limits of the intermediate aquifer is less articulated. The piezometric data collected during different campaigns allowed us to produce interpolated piezometric maps of the shallow and intermediate aquifers. The contour maps (Figure 2) illustrate the position of the excavation, which involved the removal of land attributable to shallow and intermediate aquifers for construction of the station and installation of the bypass system.

Groundwater circulation in the shallow aquifer is complex in terms of flow direction (Figure 2a). The groundwater flow is oriented mainly from SE to NW. Considering hydraulic conductivity around 10^{-7} m/s, we determined the velocity of groundwater flows in the shallow aquifer to be around 1–5 m/year. Note that the shallow aquifer changes its state from phreatic in some areas to fully confined elsewhere. The intermediate aquifer, which is constantly confined, shows a prevailing direction of groundwater flow from S to N (Figure 2b). Considering average hydraulic conductivity on the order of 10^{-4} m/s, we estimated a groundwater flow velocity around 50–100 m/year. To provide useful information for design purposes, in terms of sizing and configuration of the remediation [15], we focused our attention on the subsoil in the pilot test area. The high-resolution geological model was

constructed based on data from 17 boreholes, it covers an area of about 350 m². The stratigraphic relationships are those mentioned above (Figure 3).

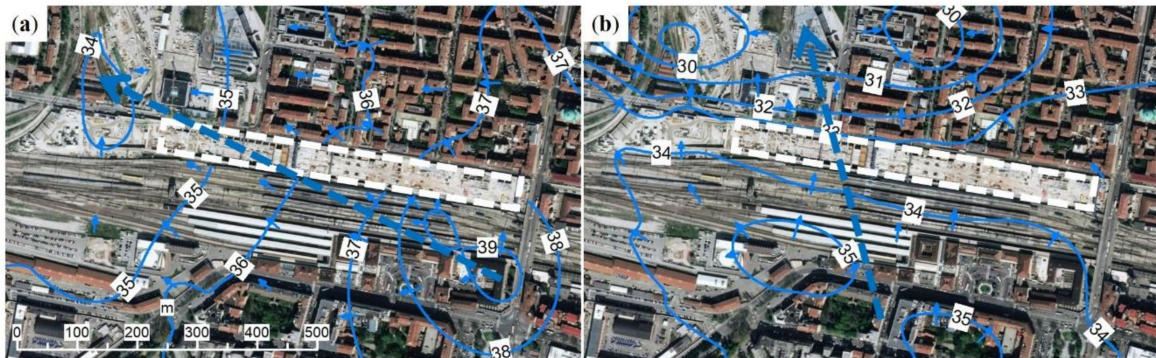


Figure 2. Representation of piezometric surface (m a.s.l.) for (a) shallow and (b) intermediate aquifer, dashed white rectangle represents excavation hosting station structure.

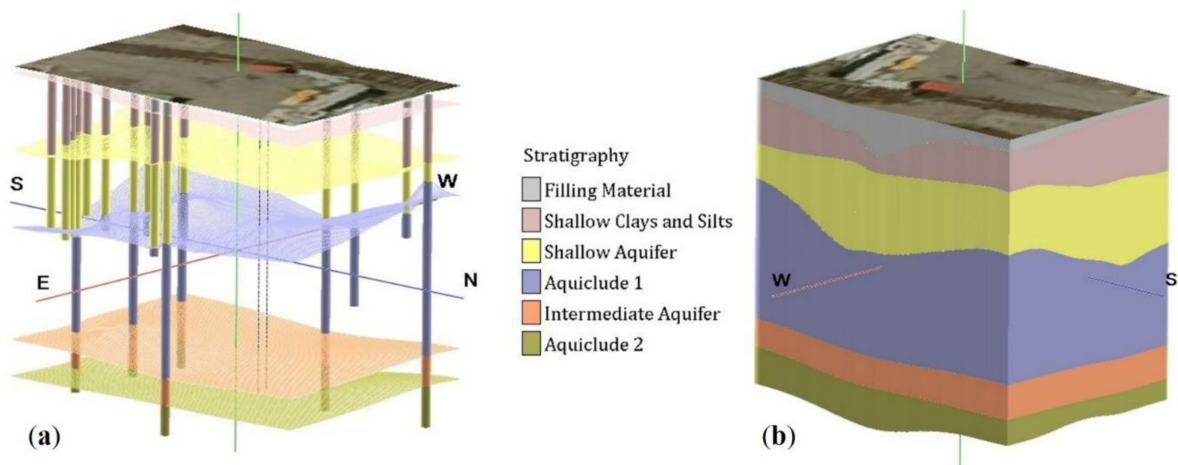


Figure 3. (a) Boreholes, stratigraphic contacts, and (b) geological model of the pilot test area in 3D.

The density of information in the pilot test area produced a stratigraphic model that identifies lateral and vertical heterogeneity. The presence of lenses with low permeability and the occurrence of preferential outflow pathways greatly influence the diffusion of contaminants and reagents and the choice/design of a remediation strategy [14]. The spatial sampling that can be achieved via direct borehole investigations is, of course, limited and cannot capture the complexity of small-scale preferential pathways [18]. On the other hand, the refinement of the geological model represents a key element for the choice and design of a technical intervention [15].

3.2. Geophysical Model

The 3D geological/hydrogeological model was refined and strengthened by integrating the geophysical evidence [22]. Geophysical investigations were carried out by performing three ERT profiles covering the area of the pilot test. The three resulting ERT sections are presented in Figure 4. A resistivity model in 3D (Figure 5) was produced by interpolation across the three ERT lines.

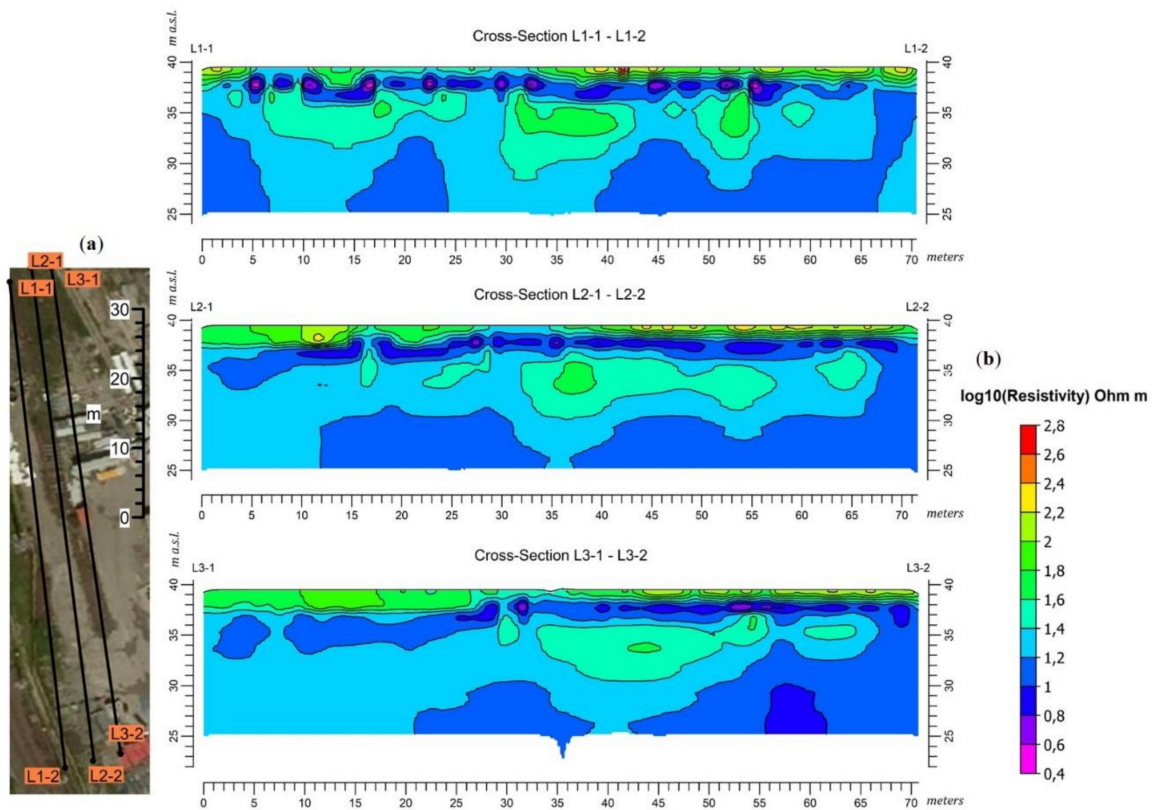


Figure 4. (a) Arrangement of electrodes in the soil in the pilot test area and (b) resulting in electrical resistivity tomography (ERT) profiles.

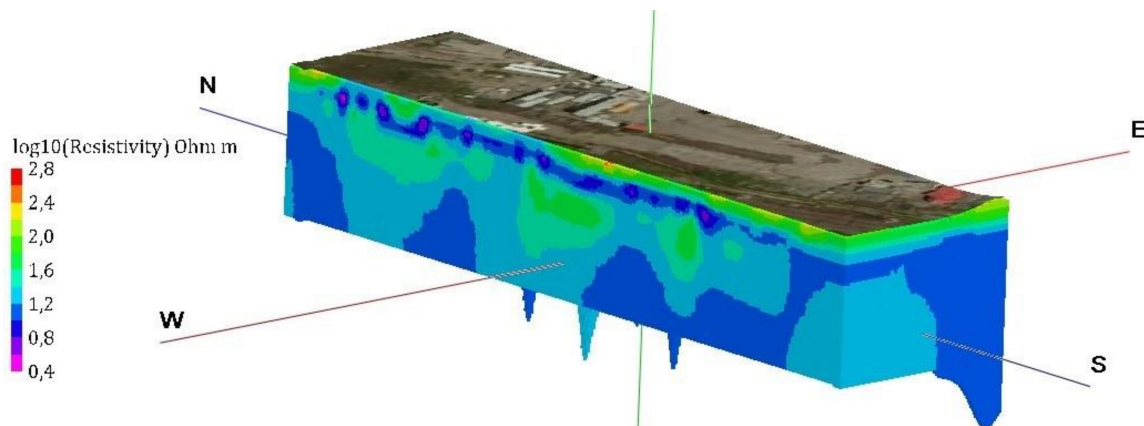


Figure 5. 3D resistivity model covering the pilot test area.

The spatial continuity of the geoelectrical data correlates high-resistivity zones with sandy deposits of the shallow aquifer, which are characterized by good hydraulic permeability. These represent preferential flow paths and transport routes, while the layers with lower resistivity correspond to clayey horizons, which feature low permeability. The use of closely spaced 2D ERT data facilitates the spatialization of data [22]. The combination of noninvasive methods with traditional and nonreplaceable punctual prospecting techniques captures the variability of geological heterogeneity and the complexity of the transport process [23]. High-resolution characterization and integration of geophysical models represent key elements for remediation design and intervention optimization [15].

3.3. Contamination Status Evolution

Figures 6 and 7 show more relevant maps for the reconstruction of the contamination status of groundwater (PCE and TCE). Tetrachloroethylene (PCE) and Trichloroethylene (TCE) were certainly used in the past as degreasing solvents and constitute the primary contaminants. Each figure shows the values of concentrations at three time instants. The contour maps illustrate some of the phases of construction of the train station. These are compatible with the phases of aquifer response to possible sources of contamination. Concentration values are compared to the Italian threshold limits (CSC): the limits between each class correspond to multiples of the CSC value for each contaminant.

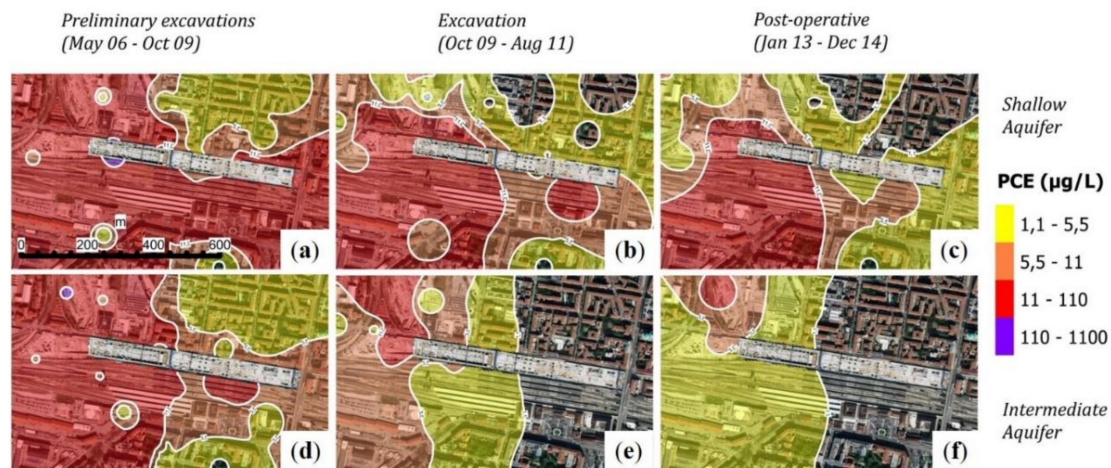


Figure 6. Contour maps representing values of tetrachloroethylene (PCE) concentration in the (a–c) shallow and (d–f) intermediate aquifers at three time instants.

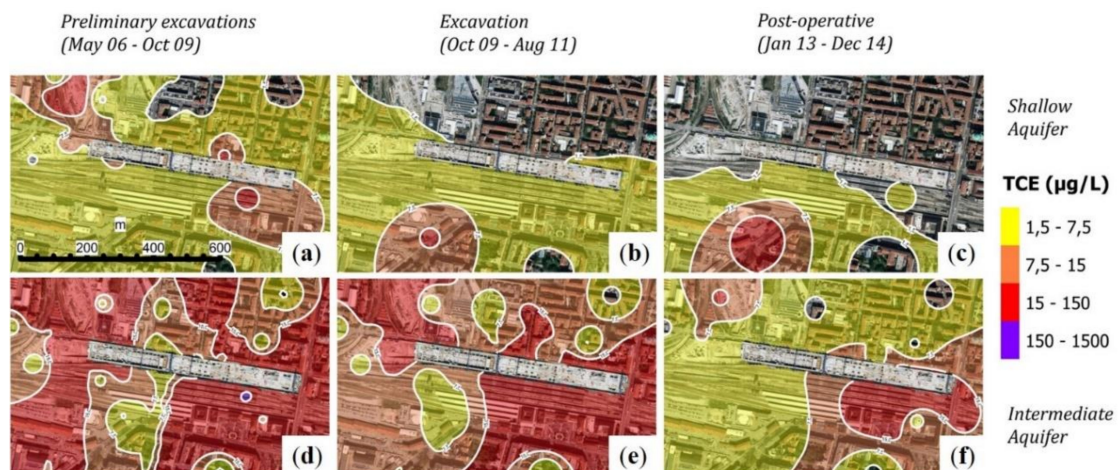


Figure 7. Contour maps representing values of trichloroethylene (TCE) concentration in (a–c) shallow and (d–f) intermediate aquifers at three time instants.

CSC excesses are concentrated during working activities in two phases: preliminary excavation and excavation. Afterwards, the contamination levels decrease in terms of both areal extension and concentration. The general evolution shows how station processing activities clearly influenced the quality of groundwater. In fact, as soon as the preliminary excavation phase ends, there is a constant amelioration of groundwater quality. Moreover, during the postoperative period, there is an improved qualitative state and it is possible to identify the areas affected by significant residual contamination [55]. The increased concentration of chlorinated solvents during the excavation phases could be related to the remobilization of contaminants adsorbed on the solid soil matrix or partly present as trapped nonaqueous phase [56].

3.4. Design of Remediation Strategy and Implementation of Pilot Test

The design of the remediation strategy should consider the specificity of the contaminated site, which can be summarized as follows:

1. A relatively large area is affected by a low concentration of contaminants.
2. Small masses of chlorinated solvents have to be treated.
3. There is thin and slow groundwater circulation in the shallow aquifer.
4. There are channelized coarse-grained sediments that can act as drains for fluids to be injected into the aquifer.

We considered the technological approaches suitable for a situation of widespread contamination with the presence of well-identified higher contamination spots. The potentially applicable technologies fall within the range of in situ interventions, both physical-chemical and biological. The applicability of technologies such as monitored natural attenuation (MNA) and enhanced natural attenuation (ENA) [57] was experimentally verified. Experimentation (not shown here) showed that natural attenuation phenomena do not allow a significant reduction of contaminants in the groundwater. However, the experiments revealed the possibility to accelerate the reductive dechlorination biological process by adding an electron donor [30]. Based on the results, biological reductive dechlorination was recognized as a potential approach for site remediation, but the extremely low chlorinated aliphatic hydrocarbon (CAH) concentration and consequent kinetic limitation made it unfeasible for the site. The possibility of using a dispersed colloidal activated carbon (PlumeStop™, Regenesis, San Clemente, CA, USA) was investigated as a site-specific remediation approach [10]. The micrometric carbon is marked by a proprietary surface-charge modification to enable dispersion and can be easily injected into a contaminated aquifer. It creates an in situ adsorption zone that can potentially reduce CAH concentration quickly. Furthermore, it raises the kinetics of the biological reduction by locally increasing the bioavailable CAH concentration at the carbon surface [11]. The technology was co-injected with an electron donor (HRC™, Regenesis, San Clemente, CA, USA) to stimulate indigenous bacteria to degrade the chlorinated compounds [12]. The intervention consists of creating an injection front corresponding to some contaminated piezometers. Based on contamination evolution, different areas for the application of PlumeStop™ and HRC™ were selected (Figure 8).



Figure 8. Identification of the pilot test and other intervention areas.

For each area, the characteristics of the aquifers to be treated and the quantities of product to be injected were identified. A multiple injection system was developed for the generation of reactive

zones [10]. Fixed stations allowed the injection of reagents at high pressure, repeated over time and at different depths along the vertical, to use selective dosing corresponding to the most contaminated zones. The treatment stations were customized depending on the type of contamination, the geological sequence, and permeability characteristics. Injections were performed at regular depth intervals, starting from the deeper portions and gradually moving toward the shallower ones, to affect the more permeable layers of the intermediate aquifer ("isolated" by an impermeable septum) first, and then the less permeable shallow aquifer. High-pressure injections traced the product's rise along with fractures and preferential flow pathways. Thus, low-pressure injections were performed to facilitate good distribution of the product into the more permeable layers. The multiple injection system was customized depending on local characteristics. For this reason, the pilot test area was investigated in detail. The ERT survey and soil and groundwater sampling confirmed satisfactory dispersion of PlumeStop™ during pilot testing. The investigations carried out with Geoprobe penetrometers verified effective diffusion of the product in the shallow aquifer. A visual comparison showed good distribution of the product, a homogeneous coating of soil particles, and evidence perceptible up to 3 meters away from the injection point. The most permeable aquifer portions (9–9.5 m from ground level) had a more evident change in color, probably due to a greater quantity of products able to permeate this zone. The passive groundwater sampling system demonstrated good distribution of the amendment in the intermediate aquifer. The geophysical surveys performed in near real time provided undoubtedly critical information, especially in terms of where and how in situ remediation actions affected different portions of the subsurface as an effect of subsoil hydraulic heterogeneity [58]. In fact, the physical variable of interest, electrical resistivity, is strongly related to state variables of key environmental interest [59]. In the case considered here, the injected solutes (PlumeStop™ and HRC™) raised the electrical conductivity of natural groundwater, as shown also by laboratory tests (not shown here). Thus, it was relatively easy to track the injected plumes by using time-lapse ERT. Figure 9 shows the results of a preliminary PlumeStop™ injection conducted in November 2015 and monitored using an ERT line corresponding to the direction of line L1 (see Figure 4a) but slightly shifted to the north. Note how the low electrical resistivity manifests itself because of PlumeStop™ injection, corresponding with the sandy bodies also identified in Figure 5. The resistivity changes are not symmetrical with respect to the injection point (blue arrow in Figure 9) because of the strong heterogeneity of the shallow aquifer. The red zones in Figure 9 indicate no resistivity changes. These zones mainly correspond to aquiclude 1, where the product could not penetrate because of the lower permeability of this formation.

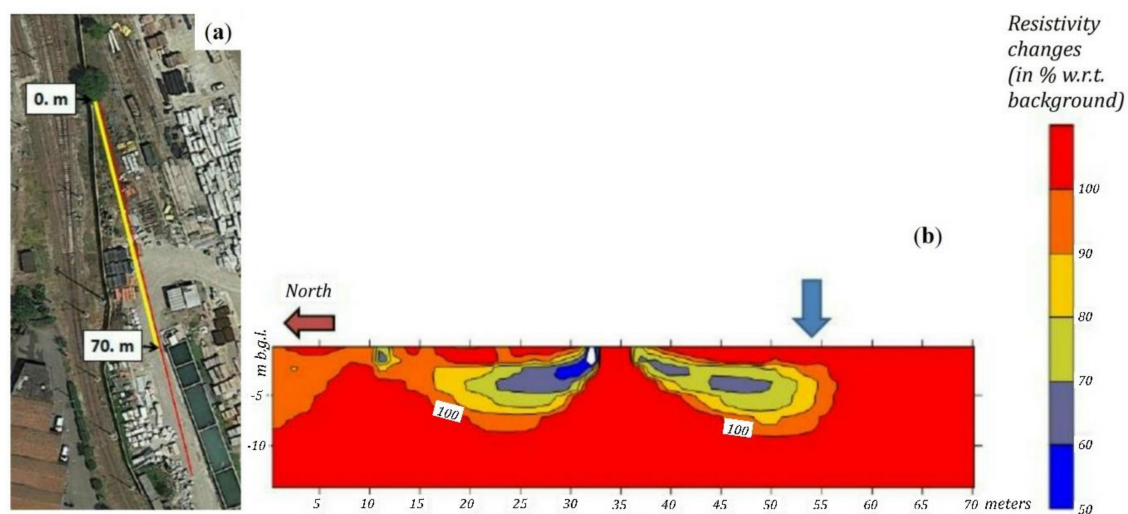


Figure 9. (a) Trace of the ERT line and (b) section illustrating resistivity changes (in % with regard to (w.r.t.) background) caused by PlumeStop™ injection. The injection point corresponds to vertical blue arrow.

The pilot test had to be representative of the process at full scale. Its implementation provided useful information about process efficiency and the actual extent of treatment, which varied depending on the site's subsurface characteristics. Analytical monitoring and integration of geophysical data during pilot test implementation facilitated the assessment of the remediation technology performance and the evaluation of possible modifications and integrations of the intervention strategy (configuration of injection points and quantity of product to be injected).

3.5. Full-scale intervention

The results obtained during the experiment supported a definitive design choice for the full-scale intervention, determined the remediation of the identified contamination areas, and allowed achievement of the objectives and closure of the project. The following graphs illustrate the results of post-treatment monitoring of some piezometers installed in the four intervention areas for a period of two years. The first series of graphs refer to the pilot test area. The graphs show a reduction in chlorinated solvents detected after full-scale intervention in shallow aquifer below the threshold limits (CSC) established by Italian law (Figure 10).

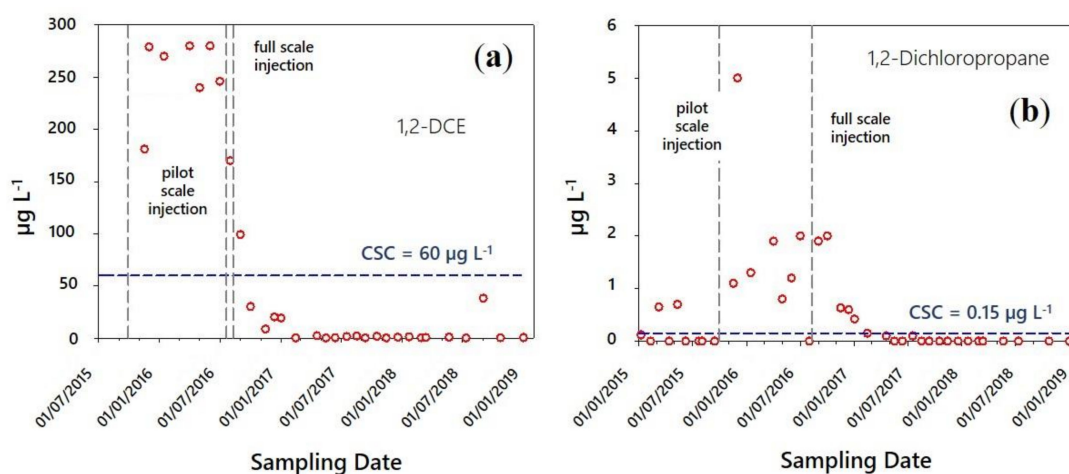


Figure 10. Concentrations of (a) 1,2 dichloroethene (1,2-DCE) and (b) 1,2-dichloropropane detected in a piezometer installed in the pilot test area.

The tendency of CAH concentrations showed a reduction to nondetectable levels within only a few weeks from application. The evolution of the concentrations of chlorinated solvents measured in some piezometers that intercepted the intermediate aquifer in intervention areas 2 and 3 are shown in Figure 11 (see Figure 8 for identification of intervention areas).

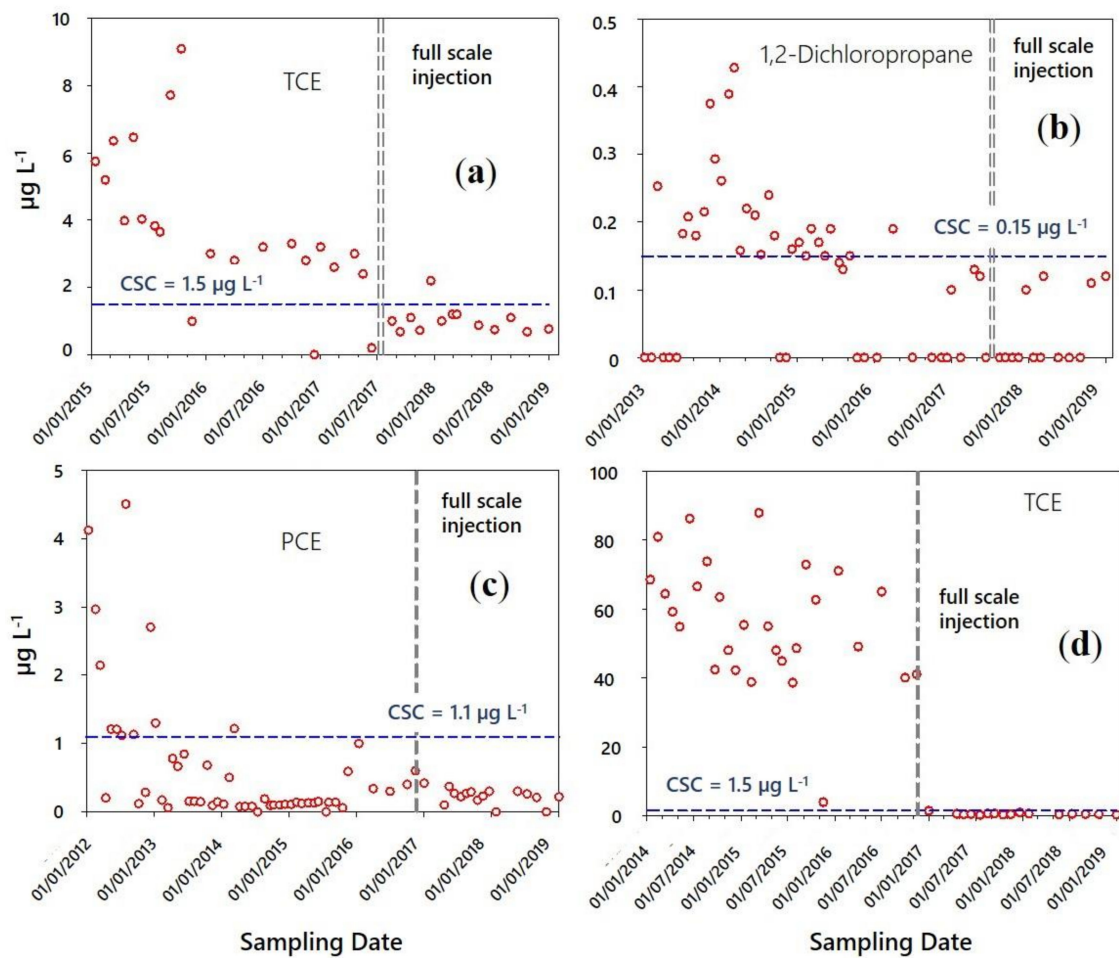


Figure 11. Concentration trend of chlorinated solvents measured in the intervention (a,b) area 2 and (c,d) area 3.

The post-intervention scenario shows a clear improvement in the state of water contamination. The concentrations detected across the piezometric network after the full-scale intervention are clearly below the remediation objectives. The parent compounds (PCE and TCE) and daughter compound (DCE) [29,30] exhibited reductions of one order of magnitude within the first month. With regard to the concentration detected in the shallow aquifer in the last area of intervention (area 4, see Figure 8), a sequential increase of DCE and vinyl chloride was observed in subsequent monitoring data (Figure 12).

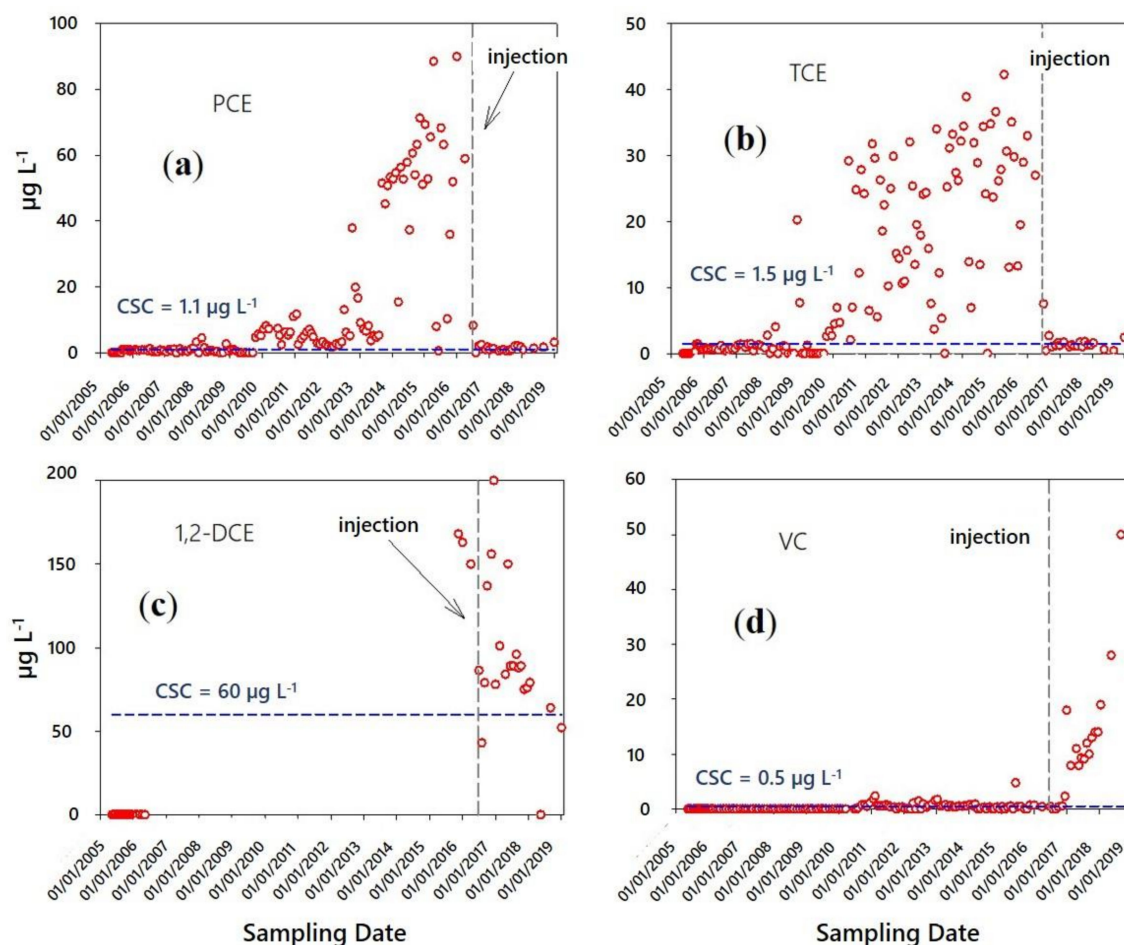


Figure 12. (a) PCE, (b) TCE, (c) 1,2-DCE, and (d) vinyl chloride (VC) concentrations detected in shallow aquifers in the last intervention area.

The last intervention area is located upstream of the railway station from a hydrogeological point of view. The increment of PCE and TCE concentration in the post-excavation phases shows that chlorinated solvents entered from areas outside the site. The injection of reagents reduced the concentration of compounds with higher numbers of chlorine atoms. The increase of DCE and VC after the injection indicates that solvent degradation proceeded without limitation despite the significant reduction of parent compounds in the aqueous phase [29,30]. Under anaerobic conditions, accumulation of cis-DCE or vinyl chloride (VC) is often observed at CAH contaminated sites [60]. Hydrogen atoms replace chlorine atoms one after the other, resulting in the typical dechlorination sequence from PCE via TCE, cis-DCE, and VC, down to ethane. The rate of reductive dechlorination decreases with the decreasing number of chloroatoms, causing an accumulation of cis-DCE or VC [60]. Compounds with a higher degree of chlorination, such as PCE and TCE, were detected at lower concentrations, presenting intense biological dechlorinating activity after the injections. Previous studies underlined that unanswered questions remain regarding the effectiveness of activated carbon-based amendments, given the lack of both field data and evidence of a biodegradation process [10]. The results obtained in the last intervention area (Figure 12) clearly highlight the occurrence and persistence of biodegradation. A combined injection of PlumeStop™ and HRC™ into groundwater represents an innovative remediation operation, the first of its kind to be realized on a large scale in European territory. Intervention monitoring played a fundamental role in validating the performance of the implemented remediation strategy. The reduction of CAH concentration below CSC limits is evidence of the effectiveness of the adopted remediation technology for abatement of chlorinated solvents, through the combined action of contaminant absorption and biodegradation processes. Based on the literature,

there is still uncertainty regarding how subsurface heterogeneity may affect the design, implementation, and monitoring of this technology [10]. The remedial investigation phase primarily focuses on characterizing subsurface geology and contaminant distribution [61]. From the implementation perspective, field applications should continuously stress adequate site characterization for remedial design. Verifying the amendment distribution should be part of performance monitoring. The distribution of activated carbon-based amendments is a key factor determining the success of the remedy [10]. The multidisciplinary geodatabase and integrated data modeling support the design, sizing, and configuration of the intervention strategy. In fact, the injection mode strongly depends on geological, hydrogeological, and operational characteristics, and particularly critical is the possible presence of preferential flow pathways. The geophysical model obtained from the three ERT profiles strengthened the geological model and provided the necessary high-resolution details. Electrical resistivity tomography measurements indicated that the geological site structure, hydrogeology, and the injected product can be discriminated based on altered electrical properties [22–24]. The realization of injection stations and the injection of PlumeStop™ were done based on the most suitable configuration. The pilot test, appropriately coordinated through the multidisciplinary and multitemporal data management model, was checked in the implementation phase in terms of yield through ERT, soil, and groundwater sampling. Geophysical surveys and monitoring activities were conducted in near real time to control the effectiveness of the intervention, in terms of the capacity of product diffusion. The field test provided an impressive picture, illustrating how in situ remediation actions affected different portions of the subsurface, as an effect of subsoil hydraulic heterogeneity. The pilot test provided the elements for verifying efficiency, optimizing the intervention layout, and designing an optimized full-scale intervention. The data-driven model comprises, collects, and establishes a connection between environmental variables, to optimize the contribution of each aspect supporting the design, implementation, and validation of the remediation technique. The hydrogeophysical model and thematic database act as integrated and continuously updated tools that can manage and calibrate the progress of the intervention modality according to innovative approaches during the remediation phases, from pilot site to full-scale intervention. The multisource model, data fusion, and integrated approach demonstrate the biodegradation process in conjunction with contaminant adsorption for in situ subsurface remediation of chlorinated solvents with activated carbons and illustrate how geological heterogeneity affects reagent distribution.

4. Conclusions

This paper presents a case of coordinated use of geological, hydrochemical, and geophysical data to support characterizing a contaminated site at high resolution, designing a remediation intervention, monitoring and validating a pilot test, and implementing an effective remediation strategy at full scale. The hydrogeophysical model and thematic database act as integrated and continuously updated tools that can optimize the investigation during the characterization phase, support the choice of strategies in the planning phase, and manage and calibrate the progress of the intervention modality according to innovative approaches during the remediation phase. Representing the geological structure with a 3D model facilitates its understanding and depicts the hydrogeological settings. The high-resolution lithostratigraphic reconstruction caught the variability of geological heterogeneities, which exert a decisive influence on the contamination dynamics and decontamination mechanisms. The combination of geophysical evidence strengthened and refined the 3D geological/hydrogeological model by providing data spatialization. The hydrogeological uniqueness and chemical peculiarities supported the selection of a remediation technology and the identification of application points. The indications acquired by the pilot test optimized the full-scale operation. Time-lapse geophysical surveys and soil and groundwater sampling during pilot testing delivered critical information, especially in terms of where and how in situ remediation actions affected different portions of the subsurface, as an effect of subsoil hydraulic heterogeneity. The operating project provided an innovative remediation strategy for sites contaminated by chlorinated DNAPLs. The remediation strategy implied the creation

of "reactive" zones capable of significantly and permanently reducing the concentration of chlorinated solvents in groundwater through the combined action of adsorption and biodegradation. The results of full-scale intervention provide evidence for intense biological dechlorinating activity. Achieving the remediation objectives and project closure is based on integrating multidisciplinary data using a multiscale approach. This research represents the first completed example in European territory of the remediation of an aquifer contaminated with chlorinated solvents by a combination of adsorption and biodegradation.

Author Contributions: Conceptualization, P.C., C.E., and M.P.P.; methodology, P.C., C.E., and M.P.P.; software, P.C. and P.V.; validation, M.P.P., C.E., P.V., J.B., and G.C.; formal analysis, M.P.P., C.E., G.C., and P.V.; investigation, J.B. and G.C.; resources, M.P.P.; data curation, P.C., M.P.P., and G.C.; writing—original draft preparation, P.C.; writing—review and editing, C.E. and G.C.; visualization, P.C.; supervision, C.E., G.C., and M.P.P.; project administration, M.P.P.

Funding: This research received no external funding.

Acknowledgments: We gratefully acknowledge Fabio Tatti, PhD, for groundwater circulation numerical modeling and Dr. Francesca Grecolini for geotechnical laboratory analyses.

Conflicts of Interest: The authors declare no conflict of interest.

References

1. Kueper, B.H.; Stroo, H.; Vogel, C.M.; Ward, C. Source Zone Remediation: The State of the Practice. In *Chlorinated Solvent Source Zone Remediation*; Kueper, B.H., Stroo, H., Vogel, C.M., Ward, C., Eds.; SERDP/ESTCP Environmental Remediation Technology; Springer: New York, NY, USA, 2014; pp. 1–27. [[CrossRef](#)]
2. McCarty, P.L. Groundwater Contamination by Chlorinated Solvents: History, Remediation Technologies and Strategies. In *In Situ Remediation of Chlorinated Solvent Plumes*; Stroo, H., Ward, C., Eds.; SERDP/ESTCP Environmental Remediation Technology; Springer: New York, NY, USA, 2010; pp. 1–28. [[CrossRef](#)]
3. Ajo-Franklin, J.B.; Geller, J.T.; Harris, J.M. A survey of the geophysical properties of chlorinated DNAPLs. *J. Appl. Geophys.* **2006**, *59*, 177–189. [[CrossRef](#)]
4. Luciano, A.; Viotti, P.; Petrangeli, P.M. Laboratory investigation of DNAPL migration in porous media. *J. Hazard. Mater.* **2010**, *176*, 1006–1017. [[CrossRef](#)]
5. Lee, K.Y.; Chrysikopoulos, C.V. Dissolution of a multicomponent DNAPL pool in an experimental aquifer. *J. Hazard. Mater.* **2006**, *128*, 218–226. [[CrossRef](#)]
6. Abdel-Moghny, T.; Mohamed, R.S.A.; El-Sayed, E.; Aly, S.M.; Snousy, M.G. Effect of Soil Texture on Remediation of Hydrocarbons-Contaminated Soil at El -Minia District, Upper Egypt. *ISRN Chem. Eng.* **2012**, *2012*, 406598. [[CrossRef](#)]
7. Fjordbøge, A.S.; Janniche, G.S.; Jørgensen, T.H.; Grosen, B.; Wealthall, G.; Christensen, A.G.; Kern-Jespersen, H.; Broholm, M.M. Integrity of Clay till Aquitards to DNAPL Migration: Assessment Using Current and Emerging Characterization Tools. *Groundw. Monit. Remediat.* **2017**, *37*, 45–61. [[CrossRef](#)]
8. Rao, P.S.C.; Annable, M.D.; Kim, H. NAPL source zone characterization and remediation technology performance assessment: Recent developments and applications of tracer techniques. *J. Contam. Hydrol.* **2000**, *45*, 63–78. [[CrossRef](#)]
9. Simon, J.A. Editor's perspective—An in situ revelation: First retard migration, then treat. *Remediation* **2015**, *25*, 1–7. [[CrossRef](#)]
10. Fan, D.; Gilbert, E.J.; Fox, T. Current state of in situ subsurface remediation by activated carbon-based amendments. *J. Environ. Manag.* **2017**, *204*, 793–803. [[CrossRef](#)] [[PubMed](#)]
11. Georgi, A.; Schierz, A.; Mackenzie, K.; Kopinke, F. Colloidal activated carbon for in-situ groundwater remediation—Transport characteristics and adsorption of organic compounds in water-saturated sediment columns. *J. Contam. Hydrol.* **2015**, *179*, 76–88. [[CrossRef](#)] [[PubMed](#)]
12. Wood, R.C.; Huang, J.; Goltz, M.N. Modeling Chlorinated Solvent Bioremediation Using Hydrogen Release Compound (HRC). *Bioremed. J.* **2006**, *10*, 129–141. [[CrossRef](#)]
13. Simpkin, T.J.; Norris, R.D. Engineering and Implementation Challenges for Chlorinated Solvent Remediation. In *In Situ Remediation of Chlorinated Solvent Plumes*; Stroo, H., Ward, C., Eds.; SERDP/ESTCP Environmental Remediation Technology; Springer: New York, NY, USA, 2010; pp. 109–143. [[CrossRef](#)]

14. Harris, M.K.; Looney, B.B.; Jackson, D.G. Geology and environmental remediation: Savannah River Site, South Carolina. *Environ. Geosci.* **2004**, *11*, 191–204. [[CrossRef](#)]
15. Suthersan, S.S.; Horst, J.; Schnobrich, M.; Welty, N.; McDonough, J. *Remediation Engineering, Design Concepts*, 2nd ed.; CRC Press: Boca Raton, FL, USA; Taylor & Francis Group: Boca Raton, FL, USA, 2016; pp. 107–135.
16. Samouelian, A.; Cousin, I.; Tabbagh, A.; Bruand, A.; Richard, G. Electrical resistivity survey in soil science: A review. *Soil Tillage Res.* **2005**, *83*, 173–193. [[CrossRef](#)]
17. Stewart, M.; North, L. A borehole geophysical method for detection and quantification of dense, non-aqueous phase liquids (DNAPL) in saturated soils. *J. Appl. Geophys.* **2006**, *60*, 87–99. [[CrossRef](#)]
18. Pharr, M.; Humphreys, G. Sampling and Reconstruction. In *Physically Based Rendering: From Theory to Implementation*; Pharr, M., Humphreys, G., Eds.; Morgan Kaufmann Publishers Inc.: San Francisco, CA, USA, 2016; pp. 322–420. [[CrossRef](#)]
19. Cassiani, G.; Binley, A.; Kemna, A.; Wehrer, M.; Orozco, A.F.; Deiana, R.; Boaga, J.; Rossi, M.; Dietrich, P.; Werban, U.; et al. Noninvasive characterization of the Trecate (Italy) crude-oil contaminated site: Links between contamination and geophysical signals. *Environ. Sci. Pollut. Res.* **2014**, *21*, 8914–8931. [[CrossRef](#)]
20. Chambers, J.E.; Loke, M.H.; Ogilvy, R.D.; Meldrum, P.I. Noninvasive monitoring of DNAPL migration through a saturated porous medium using electrical impedance tomography. *J. Contam. Hydrol.* **2004**, *68*, 1–22. [[CrossRef](#)]
21. Chambers, J.E.; Wilkinson, P.B.; Wealthall, G.P.; Loke, M.H.; Dearden, R.; Wilson, R.; Allen, D.; Ogilvy, R.D. Hydrogeophysical imaging of deposit heterogeneity and groundwater chemistry changes during DNAPL source zone bioremediation. *J. Contam. Hydrol.* **2010**, *118*, 43–61. [[CrossRef](#)]
22. Crook, N.; Binley, A.; Knight, R.; Robinson, D.A.; Zarnetske, J.; Haggerty, R. Electrical resistivity imaging of the architecture of substream sediments. *Water Resour. Res.* **2008**, *44*, W00D13. [[CrossRef](#)]
23. Binley, A.; Hubbert, S.S.; Huisman, J.A.; Revil, A.; Robinson, D.A.; Singha, K.; Slater, L.D. The emergence of hydrogeophysics for improved understanding of subsurface processes over multiple scales. *Water Resour. Res.* **2015**, *51*, 3837–3866. [[CrossRef](#)]
24. Atekwana, E.A.; Atekwana, E. A Geophysical signature of microbial activity at hydrocarbon contaminated sites: A review. *Surv. Geophys.* **2010**, *31*, 247–283. [[CrossRef](#)]
25. Artimo, A.; Saraperä, S.; Ylander, I. Methods for Integrating an Extensive Geodatabase with 3D Modeling and Data Management Tools for the Virttaankangas Artificial Recharge Project, Southwestern Finland. *Water Resour. Manag.* **2008**, *22*, 1723–1739. [[CrossRef](#)]
26. Ciampi, P.; Esposito, C.; Petrangeli Papini, M. Hydrogeochemical Model Supporting the Remediation Strategy of a Highly Contaminated Industrial Site. *Water* **2019**, *11*, 1371. [[CrossRef](#)]
27. Breunig, M.; Zlatanova, S. 3D geo-database research: Retrospective and future directions. *Comput. Geosci.* **2011**, *37*, 791–803. [[CrossRef](#)]
28. Huysegoms, L.; Cappuyns, V. Critical review of decision support tools for sustainability assessment of site remediation options. *J. Environ. Manag.* **2017**, *196*, 278–296. [[CrossRef](#)] [[PubMed](#)]
29. Aulenta, F.; Bianchi, A.; Majone, M.; Petrangeli, P.M.; Potalivo, M.; Tandoi, V. Assessment of natural or enhanced in situ bioremediation at a chlorinated solvent contaminated aquifer in Italy: A microcosm study. *Environ. Int.* **2005**, *31*, 185–190. [[CrossRef](#)]
30. Aulenta, F.; Pera, A.; Petrangeli, P.M.; Rossetti, S.; Majone, M. Relevance of side reactions in anaerobic reductive dechlorination microcosms amended with different electron donors. *Water Res.* **2007**, *41*, 27–38. [[CrossRef](#)]
31. Matturro, B.; Heavner, G.L.; Richardson, R.E.; Rossetti, S. Quantitative estimation of *Dehalococcoides mccartyi* at laboratory and field scale: Comparative study between CARD-FISH and Real Time PCR. *J. Microbiol. Methods* **2013**, *93*, 127–133. [[CrossRef](#)]
32. Bozzano, F.; Petitta, M.; Del Bon, A.; Nardoni, F.; Pacioni, E. Conceptual model and flow numerical simulation of aquifer contaminated by chlorinated solvents in Rho (MI). *Ital. J. Eng. Geol. Environ.* **2007**, *1*, 97–105. [[CrossRef](#)]
33. Cheong, J.Y.; Hamm, S.Y.; Kim, H.S.; Ko, E.J.; Yang, K.; Lee, J.H. Estimating hydraulic conductivity using grain-size analyses, aquifer tests, and numerical modeling in a riverside alluvial system in South Korea. *Hydrogeol. J.* **2008**, *16*, 1129. [[CrossRef](#)]
34. Mirus, B.B. Evaluating the importance of characterizing soil structure and horizons in parameterizing a hydrologic process model. *Hydrol. Process.* **2015**, *29*, 4611–4623. [[CrossRef](#)]

35. ASTM International. *Standard Practice for Classification of Soils for Engineering Purposes (Unified Soil Classification System)*; ASTM D2487-11; ASTM International: Montgomery County, PA, USA, 2011.
36. ASTM International. *Standard Test Methods for Liquid Limit, Plastic Limit, and Plasticity Index of Soils*; ASTM D4318-10; ASTM International: Montgomery County, PA, USA, 2010.
37. ASTM International. *Standard Test Methods for Laboratory Determination of Water (Moisture) Content of Soil and Rock by Mass*; ASTM D2216-10; ASTM International: Montgomery County, PA, USA, 2010.
38. Chidichimo, F.; De Biase, M.; Rizzo, E.; Masi, S.; Straface, S. Hydrodynamic parameters estimation from self-potential data in a controlled full scale site. *J. Hydrol.* **2015**, *522*, 572–581. [[CrossRef](#)]
39. Binley, A.; Kemna, A. DC Resistivity and Induced Polarization Methods. In *Hydrogeophysics*; Rubin, Y., Hubbard, S.S., Eds.; Water Science and Technology Library; Springer: Dordrecht, The Netherlands, 2005; Volume 50, pp. 129–156. [[CrossRef](#)]
40. Cassiani, G.; Bruno, V.; Villa, A.; Fusi, N.; Binley, A. A saline tracer test monitored via time-lapse surface electrical resistivity tomography. *J. Appl. Geophys.* **2006**, *59*, 244–259. [[CrossRef](#)]
41. Daily, W.; Ramirez, A.; Binley, A.; LeBrecque, D. Electrical resistance tomography. *Lead. Edge* **2004**, *23*, 438–442. [[CrossRef](#)]
42. Cultrera, M.; Boaga, J.; Di Sipio, E.; Dalla Santa, G.; De Seta, M.; Galgaro, A. Modelling an induced thermal plume with data from electrical resistivity tomography and distributed temperature sensing: A case study in northeast Italy. *Hydrogeol. J.* **2018**, *26*, 837. [[CrossRef](#)]
43. Hunkeler, D. Geological and Hydrogeological Characterization of Subsurface. In *Hydrocarbon and Lipid Microbiology Protocols*; McGenity, T., Timmis, K., Nogales, B., Eds.; Springer Protocols Handbooks; Springer: Berlin/Heidelberg, Germany, 2016; pp. 27–44. [[CrossRef](#)]
44. Britt, S.L.; Parker, B.L.; Cherry, J.A. A Downhole Passive Sampling System to Avoid Bias and Error from Groundwater Sample Handling. *Environ. Sci. Technol.* **2010**, *44*, 4917–4923. [[CrossRef](#)] [[PubMed](#)]
45. Deiana, R.; Cassiani, G.; Villa, A.; Bagliani, A.; Bruno, V. Calibration of a vadose zone model using water injection monitored by GPR and electrical resistance tomography. *Vadose Zone J.* **2008**, *7*, 215–226. [[CrossRef](#)]
46. Perri, M.T.; Cassiani, G.; Gervasio, I.; Deiana, R.; Binley, A. A saline tracer test monitored via both surface and cross-borehole electrical resistivity tomography: Comparison of time-lapse results. *J. Appl. Geophys.* **2012**, *79*, 6–16. [[CrossRef](#)]
47. Haaken, K.; Deidda, G.P.; Cassiani, G.; Kemna, A.; Deiana, R.; Putti, M.; Paniconi, C. Flow dynamics in hyper-saline aquifers: Hydro-geophysical monitoring and modelling. *Hydrol. Earth Syst. Sci.* **2017**, *21*, 1439–1454. [[CrossRef](#)]
48. Lekula, M.; Lubczynski, M.W.; Shemang, E.M. Hydrogeological conceptual model of large and complex sedimentary aquifer systems—Central Kalahari Basin. *Phys. Chem. Earth* **2018**, *106*, 47–62. [[CrossRef](#)]
49. Kaliraj, S.; Chandrasekar, N.; Peter, T.S.; Selvakumar, S.; Magesh, N.S. Mapping of coastal aquifer vulnerable zone in the south west coast of Kanyakumari, South India, using GIS-based DRASTIC model. *Environ. Monit. Assess.* **2015**, *187*, 4073. [[CrossRef](#)]
50. Safarbeiranvand, M.; Amanipoor, H.; Battaleb-Looie, S.; Ghanemi, K.; Ebrahimi, B. Quality Evaluation of Groundwater Resources using Geostatistical Methods (Case Study: Central Lorestan Plain, Iran). *Water Resour. Manag.* **2018**, *32*, 3611–3628. [[CrossRef](#)]
51. Mirzaei, R.; Sakizadeh, M. Comparison of interpolation methods for the estimation of groundwater contamination in Andimeshk-Shush Plain, Southwest of Iran. *Environ. Sci. Pollut. Res.* **2016**, *23*, 2758–2769. [[CrossRef](#)] [[PubMed](#)]
52. Adhikary, P.P.; Dash, C.J. Comparison of deterministic and stochastic methods to predict spatial variation of groundwater depth. *Appl. Water Sci.* **2017**, *7*, 339–348. [[CrossRef](#)]
53. Lugli, S.; Marchetti Dori, S.; Fontana, D.; Panini, F. Composizione dei sedimenti sabbiosi nelle perforazioni lungo il tracciato ferroviario ad alta velocità: Indicazioni preliminari sull'evoluzione sedimentaria della media pianura modenese. *Ital. J. Quat. Sci.* **2004**, *17*, 379–389.
54. Emilia-Romagna, R.; Di Dio, G. *Riserve Idriche Sotterranee Della Regione Emilia-Romagna*; SELCA: Firenze, Italy, 1998; p. 120.
55. Leharne, S. Transfer phenomena and interactions of non-aqueous phase liquids in soil and groundwater. *ChemTexts* **2019**, *5*, 5. [[CrossRef](#)]
56. Tatti, F.; Petrangeli, P.M.; Raboni, M.; Viotti, P. Image analysis procedure for studying Back-Diffusion phenomena from low-permeability layers in laboratory tests. *Sci. Rep.* **2016**, *6*, 30400. [[CrossRef](#)]

57. Declercq, I.; Cappuyns, V.; Duclos, Y. Monitored natural attenuation (MNA) of contaminated soils: State of the art in Europe—A critical evaluation. *Sci. Total Environ.* **2012**, *426*, 393–405. [[CrossRef](#)] [[PubMed](#)]
58. Vereecken, H.; Binley, A.; Cassiani, G.; Revil, A.; Titov, K. Applied Hydrogeophysics. In *Applied Hydrogeophysics*; Vereecken, H., Binley, A., Cassiani, G., Revil, A., Titov, K., Eds.; NATO Science Series; Springer: Dordrecht, The Netherlands, 2006; Volume 71, pp. 1–22. [[CrossRef](#)]
59. Lesmes, D.P.; Friedman, S.P. Relationships between the Electrical and Hydrogeological Properties of Rocks and Soils. In *Hydrogeophysics*; Rubin, Y., Hubbard, S.S., Eds.; Water Science and Technology Library; Springer: Dordrecht, The Netherlands, 2005; Volume 50, pp. 87–128. [[CrossRef](#)]
60. Tiehm, A.; Schmidt, K.R. Sequential anaerobic/aerobic biodegradation of chloroethenes-aspects of field application. *Curr. Opin. Biotechnol.* **2011**, *22*, 415–421. [[CrossRef](#)]
61. Kueper, B.H.; Davies, K.L. DNAPL source zone characterization and delineation. In *Chlorinated Solvent Source Zone Remediation*; Kueper, B.H., Stroo, H., Vogel, C.M., Ward, C., Eds.; SERDP/ESTCP Environmental Remediation Technology; Springer: New York, NY, USA, 2014; pp. 63–82.



© 2019 by the authors. Licensee MDPI, Basel, Switzerland. This article is an open access article distributed under the terms and conditions of the Creative Commons Attribution (CC BY) license (<http://creativecommons.org/licenses/by/4.0/>).